IEEE Access
Multidisciplinary | Rapid Review | Open Access Journal

Received November 7, 2019, accepted December 15, 2019, date of publication December 23, 2019, date of current version January 3, 2020.

Digital Object Identifier 10.1109/ACCESS.2019.2961366

Outage Throughput Capacity of Hybrid Wireless Networks Over Fading Channels

XIN WANG, ZIKAI WANG, AND QILIAN LIANG, (Fellow, IEEE)
Department of Electrical Engineering, The University of Texas at Arlington, Arlington, TX 76019, USA
Corresponding author: Zikai Wang (zikai.wang@mavs.uta.edu)

ABSTRACT How much information can be transported, i.e., the transmission rate, is a subject of great interest in hybrid wireless networks. The main focus of this paper is the effect of channel fading in hybrid wireless network, in which a wired network of base stations is deployed to support long-range communications between wireless nodes. Two types of transmission mode in hybrid wireless network, i.e., intra-cell mode and infrastructure mode, are considered. To effectively overcome fading impairment, optimal multiple access technique is applied, allowing opportunistic sources to transmit concurrently with the scheduled source. Those different sources, much like in wideband CDMA system, share the entire bandwidth. A successive interference cancellation (SIC) strategy is then introduced at receiver side to limit the intra-cell interference and achieve the maximum capacity. Meanwhile, frequency reuse scheme is employed to minimize the inter-cell interference. Since the outage capacity over different fading channels will exhibit different asymptotic behaviors, in this paper we examine the Rayleigh, Rician and Nakagami-m models, which are the most commonly used fading models. Close-form solutions for outage throughput capacity at high signal-to-noise-plus-interference ratio (SNIR) are derived. It is showed that, with opportunistic sources, the intra-cell mode effectively combats fading as wireless nodes increases; however, the infrastructure mode is bottlenecked by the downlink transmission since base station is the only transmitter in the cell during the downlink phase. The theoretical bounds obtained and proofs are instrumental to the future network modeling and design.

INDEX TERMS Hybrid wireless networks, infrastructure, fading, outage throughput capacity, opportunistic communication.

I. INTRODUCTION

Hybrid wireless network [4] combines wireless ad-hoc network nodes and base stations, as shown in Figure 1. In wireless networks, information is exchanged between different nodes over a common wireless channel. And a wired backbone provides connectivity between base stations. Different constraint, such as transmission power and bandwidth, will result in different throughput capacity during the transmission, as well as the number of the nodes in the network. Hence the key question here, is how those constraints affect the throughput capacity.

In [5], the authors initiated the study of scaling laws in large ad-hoc wireless networks. It has been illustrated that the throughput of the network decreased at $\Theta(\frac{1}{\sqrt{n}})$ as the number of nodes tends to infinity if all nodes are placed optimally and will decay at $\Theta(\frac{1}{\sqrt{n\log n}})$ if the nodes are placed randomly.

However, in [6], the authors have showed that a rate higher than $\Theta(\frac{1}{\sqrt{n}})$ is possibly achievable if we adopt a more general information theory setting. The authors of [7] have shown that for a network with randomly placed nodes, the per-node capacity has a lower bound of $\frac{1}{\sqrt{n}}$ if applying the percolation theory.

Note that the above mentioned literatures mainly focus on static wireless nodes under typical communication scenarios. In [8], the authors have shown that the network capacity can be increased if the nodes are mobile and the per-node throughput the network is kept constant even as the number of nodes n increases. In [9], the authors indicated the throughput capacity of ad-hoc networks with mobile relays. Meanwhile, the authors of [10] has shown that the same per-node throughput is achievable if more intelligent node cooperation and distributed MIMO communication on static nodes are used.

The associate editor coordinating the review of this manuscript and approving it for publication was Jinhwan Koh.

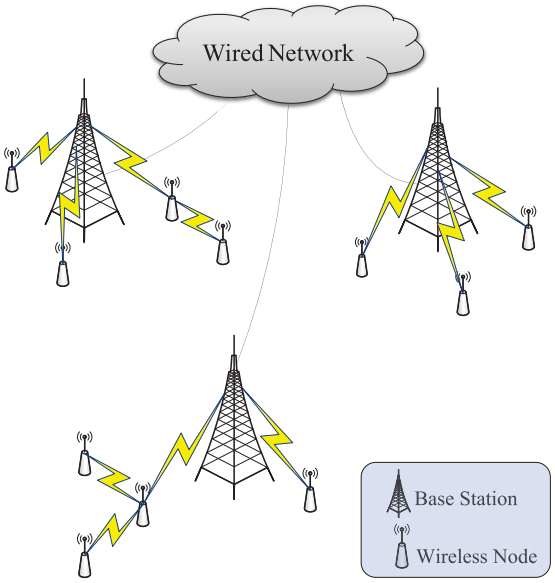

FIGURE 1. A hybrid wireless network.

Some other studies that considers different type of data traffic, such as multi-cast, can been found in [11]– [15].

The capacity of the hybrid wireless network is also a topic of great interest, and has been studied by the authors of [16]– [23]. For a two-dimensional hybrid network with b stations, the maximum per-node capacity scales as $\Theta(b/n)$ if the number of base stations increases at a speed asymptotically faster than $\sqrt{n}$ [16]. Similarly, the authors of [20] have shown that a network with wired infrastructure could achieve a per-node capacity of $\Omega(min(b/n, 1/\log b))$. Otherwise, the percolation theory [7] should be applied to achieve the maximum capacity.

In this paper, we indicate the per-node throughput capacity in the hybrid wireless networks over fading channels. Three commonly used fading models, i.e., Rayleigh, Rician and Nakagami-m fading, are demonstrated in order to analyze their effect on hybrid wireless network. Rayleigh fading model is used when antenna receives a large number of reflected and scattered waves caused by multi-path reception. While in Rician fading model, a strong dominant component is considered besides the scattered waves. Nakagami fading occurs for multi-path scattering with relatively large delay-time spreads, with different clusters of reflected waves. Unlike the previous studies, an optimal multiple access technique is applied to increase the throughput capacity of the network. Specifically, while the scheduled source is transmitting data, a set of nodes within the same cell of the source node will be selected to transmit at the same instant if such transmissions won't impair with the scheduled source. At the destination node, instead of decoding each node treating all transmissions from other nodes as interference, at the reception, after one node is decoded, its signal will be removed from the aggregate received signal before the next node is decoded. The successive interference cancellation (SIC) scheme [25], [26] is applied to do so. These selected nodes are called opportunistic sources and the bandwidth will be shared by all these nodes, like in wideband CDMA systems. Not only does this save the battery power of the nodes, it also increase the system capacity with limited interference. Previous studies on the improvement in transmission capacity with SIC could be found in [27]–[29].

Similar to [10], [19], the key idea behind our decoding scheme is that we believe the physical model used by many literatures, for example [5], [16], is somewhat strict. Specifically, this model assumes that the signals received from nodes other than the transmitter are all treated as interference. Thus long range point-to-point communication between nodes is not preferable. The optimal strategy is then to confine the transmission to nearest neighbor nodes and rely on a spatial reuse to maximize the number of simultaneous transmission. However, we take a weak restriction by means of allowing nodes to transmit data directly to their destinations in this paper. As mentioned above, opportunistic sources are selected to transmit simultaneously and with SIC decoding technique, the interference from these sources now become valuable information and the spatial multiplexing gain can then be achieved. One step further, we replace the long range wireless communications with the wired infrastructure network in order to inherit the benefit of the spatial reuse.

The rest of this paper is organized as follows. In Section II, we formulate the network model. The main contributions are given in Section III. The principle of opportunistic communication and frequency reuse is discussed in Section IV. In Section V and Section VI, we derived the outage throughput capacity for both intra-cell mode and infrastructure mode. Finally, we concludes our work in Section VII.

II. MAIN RESULTS

We consider a hybrid wireless networks with two modes, hybrid network mode and transmission mode. The details of each mode were described in [1].

For a hybrid wireless network with n nodes and b base stations while $b = o(\frac{n}{\log n})$, its outage throughput capacity over three different fading models are concluded as follows

Theorem 1:

For a network under *intra-cell* transmission mode, the per-node outage throughput capacity over ***Rayleigh*** fading is

$$T_{intra}^{Ray}(n, b) = O\left(\log(\epsilon^{\frac{b}{n}} \frac{n}{b}) W_1 \right) bit/s; \tag{1}$$

Similarly, for *infrastructure* transmission mode,

$$T_{infra}^{Ray}(n, b) = \Theta\left(\frac{b}{n} \log(\epsilon \frac{n}{b}) W_2 \right) bit/s. \tag{2}$$

where W_1 and W_2 are the bandwidth of *intra-cell* transmission mode and *infrastructure* transmission mode.

Theorem 2: For a network under*intra-cell* transmission mode, the per-node outage throughput capacity over ***Rician***

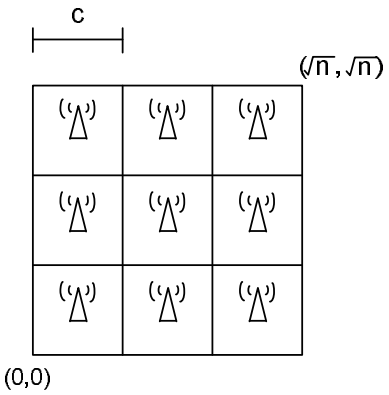

FIGURE 2. A network of size $\sqrt{n} \times \sqrt{n}$ is partitioned into b cells with side length $\sqrt{\frac{n}{b}}$.

fading is

$$T_{intra}^{Rician}(n,b) = O\left(\log[(e^{\frac{s^2}{\delta^2}}\epsilon)^{\frac{b}{n}}\frac{n}{b}]\, W_1\right) bit/s, \quad (3)$$

where s^2 and δ^2 are the direct power and scatter power of Rician fading, respectively.

Similarly, for *infrastructure* transmission mode,

$$T_{infra}^{Rician}(n,b) = \Theta\left(\frac{b}{n}\log(e^{\frac{s^2}{\delta^2}}\epsilon\frac{n}{b})\, W_2\right) bit/s. \quad (4)$$

Theorem 3: For a network under*intra-cell* transmission mode, the per-node outage throughput capacity over ***Nakagami-m*** fading is

$$T_{intra}^{Nak}(n,b) = O\left(\log[(\epsilon^{\frac{1}{m}})^{\frac{b}{n}}\frac{n}{b}]\, W_1\right) bit/s, \quad (5)$$

where m is the shape parameter of Nakagami-m fading.

Similarly, for *infrastructure* transmission mode,

$$T_{infra}^{Nak}(n,b) = \Theta\left(\frac{b}{n}\log(\epsilon^{\frac{1}{m}}\frac{n}{b})\, W_2\right) bit/s. \quad (6)$$

A. THE NUMBER OF NODES PER CELL

To identify the number of nodes in each cell, we implement the following lemma.

Lemma 4: For a network with cells of side length $c = \sqrt{n/b}$ and number of base stations $b = o(\frac{n}{\log n})$ as shown in Figure 2, the number of nodes within each cell n_c is bounded by $\Theta(\frac{n}{b})$ as $n \to \infty$.

Proof: Let A denotes the event that node i, $1 \le i \le n$, will fall into a particular cell of area c^2. Obviously, A is a Bernoulli event. Take in the assumption that all nodes are placed uniformly, we have $P_A = \frac{n/b}{n} = \frac{1}{b}$. Hence the number of nodes per cell n_c is binomial distributed with parameters $(n, \frac{1}{b})$. By applying Chernoff bound, the following inequality can be drawn

$$Pr(n_c > k_1\frac{n}{b}) \le \frac{E\{\exp(n_c)\}}{\exp(\frac{k_1 n}{b})}$$

where k_1 is a constant. Since $E\{\exp(n_c)\} = (1+(e-1)P_A)^n \le \exp[(e-1)\frac{n}{b}]$ (implementing $1 + x \le exp(x)$), we arrive at

$$Pr(n_c > k_1\frac{n}{b}) \le \exp\left\{-\frac{n}{b}[k_1 - (e-1)]\right\}. \quad (7)$$

As long as $k_1 > e-1$, according to Boole's inequality, the probability that some cells have more than $\frac{k_1 n}{b}$ nodes converges to zero as $n \to \infty$ [3].

Similarly, we have

$$Pr(n_c < k_2\frac{n}{b}) \le \frac{E\{\exp(-n_c)\}}{\exp(\frac{-k_2 n}{b})}$$

where k_2 is another constant. Since $E\{\exp(-n_c)\} = (1 + (e^{-1}-1)P_A)^n \le \exp[(e^{-1}-1)\frac{n}{b}]$, we obtain

$$Pr(n_c < k_2\frac{n}{b}) \le \exp\left\{-\frac{n}{b}[(1-e^{-1}) - k_2]\right\}. \quad (8)$$

As long as $k_2 < 1 - e^{-1}$, according to Boole's inequality, the probability that some cells have more than $\frac{k_2 n}{b}$ nodes converges to zero as $n \to \infty$. We can then conclude the above bound. ■

B. OPPORTUNISTIC COMMUNICATION

Within each cell, nodes are time-sharing and transmit in a round robin fashion. During the transmission, the scheduled source node i will be assigned for a bandwidth of W_1/n_c Hz. Then, in order to do reliable communication between node i and the destination node j, the maximum achievable rate will be [25]

$$\log\left(1 + \frac{P \cdot l(|X_i - X_j|) \cdot |h_{ij}|^2}{\mu W_1 N_0}\right) bit/s/Hz, \quad (9)$$

where μ is the fraction of the bandwidth that source node i is assigned over the entire bandwidth W_1.

It's clear that the capacity of AWGN and fading channel are conceptual different. Hence an alternative measurement, ϵ-*outage capacity* C_ϵ, is introduced for fading channel scenario. The ϵ-*outage capacity* is the largest transmission rate which satisfies $P_{out} < \epsilon$, where P_{out} is the outage probability.

Assume that data is encoded at transmitter side at a rate of R bit/s/Hz, the system is considered *in outage* if $\log\left(1 + \frac{P \cdot l(|X_i - X_j|) \cdot |h_{ij}|^2}{\mu W_1 N_0}\right) < R$. The related outage probability is

$$P_{out} = Pr\left\{\log(1 + \frac{P \cdot l(|X_i - X_j|) \cdot |h_{ij}|^2}{\mu W_1 N_0}) < R\right\}. \quad (10)$$

Solving $P_{out} = \epsilon$ yields

$$C_\epsilon = \log\left(1 + F^{-1}(\epsilon)\frac{P \cdot l(|X_i - X_j|)}{\mu W_1 N_0}\right) bit/s/Hz, \quad (11)$$

where F^{-1} is the inverse cumulative distribution function (CDF) of $|h_{ij}|^2$.

Let ρ_{od} denotes the distance between the scheduled node and destination node j, ρ_{id}, $i = 1, 2, ..., \kappa$, denote the distances between other nodes and destination node.

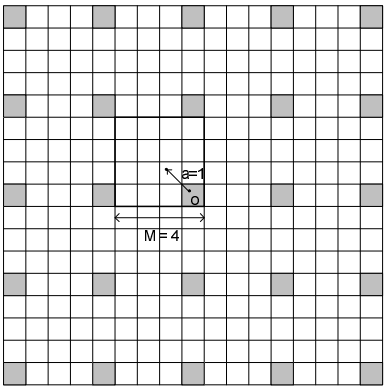

FIGURE 3. A frequency reuse scheme of a=1 where the shaded squares share the same frequency.

Without loss of generality, we assume that $\rho_{0d} \leq \rho_{1d} \leq \cdots \leq \rho_{\kappa d}$. The SIC decoding scheme could maximize the sum rate while the following set of sum rate satisfied

$$\begin{aligned} R_0 &\leq \log\left(1+\frac{P\cdot l(|X_0-X_j|)\cdot|h_{0j}|^2}{W_1N_0}\right)\\ R_0+R_1 &\leq \log\left(1+\frac{\sum_{i=0}^{1}P\cdot l(|X_i-X_j|)\cdot|h_{ij}|^2}{W_1N_0}\right)\\ &\vdots\\ \sum_{i=0}^{\kappa}R_i &\leq \log\left(1+\frac{\sum_{i=0}^{\kappa}P\cdot l(|X_i-X_j|)\cdot|h_{ij}|^2}{W_1N_0}\right), \end{aligned} \tag{12}$$

where R_i is the achievable rate of the ith node. Notice that μ is omitted from the denominator since each source node spreads its signal over the entire bandwidth.

Now we introduce the following lemmas.

Lemma 5: Given a pair of source node and destination node in any cell, the number of nodes in the same cell that have greater distance from the destination node than the source node is $\kappa = \Theta(\frac{n}{b})$.

The detailed proof could be found in [19].

Lemma 6: For any integer $a > 0$, there exists a reuse policy with M^2 frequency bands while all cells can transmit at the same time with bounded interferences, where M^2 is the *frequency reuse factor* and $M = 2(a+1)$.

The proof was provided in [2]. A frequency reuse scheme is shown in Figure 3.

Since there are $\kappa = \Theta(\frac{n}{b})$ nodes that satisfy $\rho_{0d} \leq \rho_{1d} \leq \cdots \leq \rho_{\kappa d}$, the sum rate in (12) is achievable.

III. OUTAGE THROUGHPUT CAPACITY UNDER INTRA-CELL TRANSMISSION MODE

Applying the spatial/ temporal schemes and the SIC decoding scheme, the bandwidth assigned to a scheduled source node is $\eta W_1 = \frac{1-\theta}{M^2}W_1$ Hz for intra-cell mode. The following Lemma gives the sum rate of the scheduled and opportunistic sources over Rayleigh fading channels.

Lemma 7: While under *Rayleigh* fading, as $n \to \infty$, the transmission rate of intra-cell mode from source node i to destination node j can be evaluated as follow

$$R_{intra}^{Ray} = O\left(\log(\epsilon^{\frac{b}{n}}\frac{n}{b})\right)\ bit/s/Hz, \tag{13}$$

where ϵ is the outage probability. The outage performance is

$$P_{out} = Pr\left\{||h||^2 < \frac{(2^R-1)(W_1N_0+I)}{P\cdot min(1,\rho_{0d}^{-\alpha}e^{-\gamma\rho_{0d}})}\right\}, \tag{14}$$

where $||h||^2 = \sum_{i=0}^{\kappa}|h_{ij}|^2$. Notice that $l(|X_i-X_j|) = min(1,\rho_{0d}^{-\alpha}e^{-\gamma\rho_{0d}})$ follows the large-scale radio attenuation function.

The outage capacity over Rayleigh fading is

$$C_{\epsilon}^{Ray} = \log\left\{1+\epsilon^{\frac{1}{\kappa+1}}\cdot[(\kappa+1)!]^{\frac{1}{\kappa+1}}\cdot SNIR\right\}. \tag{15}$$

Proof: The proof was provided in [1]. ■

With Lemma 7, we can now working on the first part of Theorem 1. Since the outage throughput capacity per node $T_{\epsilon}(n,b)$ is determined by the product of the allocated bandwidth and the sum rate, i.e., $\eta W_1 \cdot R_{intra}^{Ray}$, the following equation can be drawn

$$T_{intra}^{Ray}(n,b) = O\big(\log(\epsilon^{\frac{b}{n}}\frac{n}{b})\,W_1\big)\ bit/s. \tag{16}$$

The first part of Theorem 1 follows.

Similarly, we could prove the first part of Theorem 2 and Theorem 3 by introducing the following lemmas:

Lemma 8: While under *Rician* fading, as $n \to \infty$, the transmission rate of intra-cell mode from source node i to destination node j can be evaluated as follow

$$R_{intra}^{Rician} = O\left(\log[(e^{\frac{s^2}{\delta^2}}\epsilon)^{\frac{b}{n}}\frac{n}{b}]\right)\ bit/s/Hz. \tag{17}$$

Proof: see *Appendix A*. ■

Lemma 9: While under *Nakagami-m* fading, as $n \to \infty$, the transmission rate of intra-cell mode from source node i to destination node j can be evaluated as follow

$$R_{intra}^{Nak} = O\left(\log[(\epsilon^{\frac{1}{m}})^{\frac{b}{n}}\frac{n}{b}]\right)\ bit/s/Hz. \tag{18}$$

Proof: see *Appendix B*. ■

Now let's examine the impact of fading on the throughput capacity under intra-cell transmission mode. As is known, the AWGN capacity for the intra-cell transmission (without fading) is

$$C_{Awgn} = \log\big\{1+(\kappa+1)\cdot SNIR\big\}. \tag{19}$$

First, we compare the outage capacity over Rayleigh fading (15) with the AWGN capacity (19). We conclude that as $n \to \infty$, which means $\kappa \to \infty$, the fading impairment will be eliminated, since the negative influence of outage probability ϵ is weakened by $\frac{1}{\kappa+1}$ and the factor $[(\kappa+1)!]^{\frac{1}{\kappa+1}} \sim \Theta(\kappa+1)$.

Our conclusion is verified by the following simulation. In Figure 4, as κ increases, the impairment of Rayleigh fading, characterized by outage probability ϵ, is weakened and the outage capacity over Rayleigh fading asymptotically

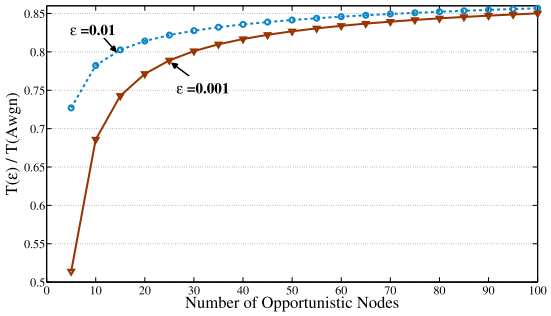

FIGURE 4. Outage throughput capacity over Rayleigh fading as a fraction of AWGN throughput capacity.

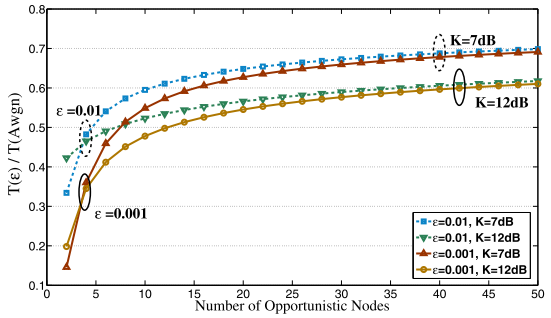

FIGURE 5. Outage throughput capacity over Rician fading as a fraction of AWGN throughput capacity.

approaches AWGN capacity. These conclusions demonstrate that the intra-cell mode could effectively combat the impact of Rayleigh fading with opportunistic sources.

The outage throughput capacity of Rician fading with different outage probability ϵ and Rician factor K is shown in Figure 5. Clearly, as opportunistic sources number κ increases, the impairment of fading is weakened. However, as κ increases, the outage throughput capacity with $K = 7$dB outperforms the scenario when $K = 12$dB. To explain this phenomenon, let us examine the derived transmission rate (30) and the related asymptotic behavior (17). Note that, on the one hand, the negative influence of outage property ϵ is mitigated by the exponent $\frac{1}{\kappa+1}$; on the other hand, the benefit of LOS transmission e^{s^2/δ^2} of Rician fading is alleviated by the exponent $\frac{1}{\kappa+1}$ as κ increases, which means the benefit of LOS transmission of all sources are offset by themselves. Nevertheless, the scatter power δ^2 in (30) will not be affected by increasing opportunistic sources. Hence, if the Rician factor K is large, the scatter power δ^2 is very small, which definitely degrades the throughput performance as shown in Figure 5.

Finally, we will discuss the intra-cell throughput performance over Nakagami-m fading. From the asymptotic behavior of transmission rate (18), since the outage ϵ is alleviated by the exponent $\frac{1}{m}$, large m will bring better throughput capacity. This conclusion is validated in Figure 6. It also demonstrates that no matter which m is chosen, intra-cell mode could effectively combat the impact of Nakagami-m fading with opportunistic sources.

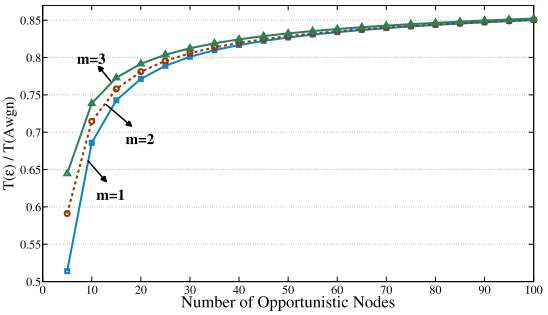

FIGURE 6. Outage throughput capacity over Nakagami-m fading as a fraction of AWGN throughput capacity ($\epsilon = 0.001$).

IV. OUTAGE THROUGHPUT CAPACITY UNDER INFRASTRUCTURE TRANSMISSION MODE

Infrastructure mode is another scenario where the data transmission happens between the nodes from different cells. To be more specific, the source nodes first relay all of their traffic to the base station of that cell during uplink phase. Subsequently, the base station decodes the transmitted data from each source node and send them through the wired infrastructure to the destination cell during the transport phase. Finally, the base station delivers data to destination node during the downlink phase.

Lemma 10: While under *Rayleigh* fading, as $n \to \infty$, the transmission rate of infrastructure mode from source node i to destination node j can be evaluated as follow

$$R_{infra}^{Ray} = \Theta\left(\log(\epsilon\frac{n}{b})\right) \ bit/s/Hz. \tag{20}$$

The proof is provided in [1]. Note that as a result of applying SIC strategy, all nodes from the same cell will share the bandwidth of $\frac{W_1}{M^2}$ during the uplink phase while during the downlink transmission, each node only gains $\frac{W_2}{M^2 n_c}$ bandwidth as the bandwidth $\frac{W_2}{M^2}$ is partitioned to n_c nodes. This bandwidth limitation further verifies the the bottleneck of downlink transmission. Hence, the outage throughput capacity of the infrastructure mode, which is determined by the downlink transmission, is $T_{infra}^{Ray}(n,b) = \lambda W_2 \cdot R_{infra}^{Ray} = \Theta\left(\frac{b}{n}\log(\epsilon\frac{n}{b})W_2\right) \ bit/s$. Then the second part of Theorem 1 follows.

Similarly, we could prove the second part of Theorem 2 and Theorem 3 by introducing the following lemmas:

Lemma 11: While under *Rician* fading, as $n \to \infty$, the transmission rate of infrastructure mode from source node i to destination node j can be evaluated as follow

$$R_{infra}^{Rician} = \Theta\left(\log(e^{\frac{s^2}{\delta^2}}\epsilon\frac{n}{b})\right) \ bit/s/Hz. \tag{21}$$

Proof: This lemma can be proved using the similar method as Lemma 10. If channel h_{bj} follows Rician fading, $|h_{bj}|^2$ follows *noncentral* χ^2 distribution with 2 degrees of

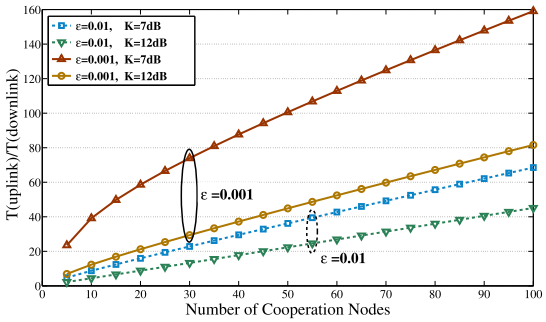

FIGURE 7. Ratio between the uplink and downlink throughput capacity under infrastructure mode over Rician fading.

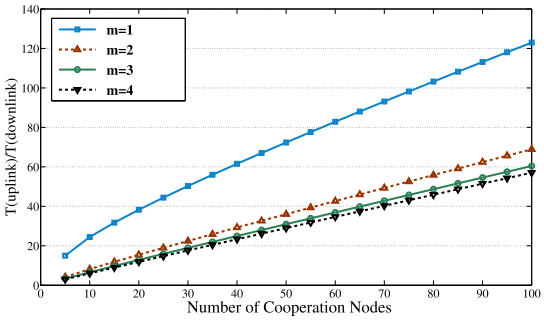

FIGURE 8. Ratio between the uplink and downlink throughput capacity under infrastructure mode over Nakagami-m fading ($\epsilon = 0.001$).

freedom. The outage capacity can be derive as:

$$C_{\epsilon}^{Rician'} = \log\left\{1 + e^{\frac{s^2}{\delta^2}} \cdot \delta^2 \cdot \epsilon \cdot SNIR'\right\} \tag{22}$$

where $SNIR' = \frac{P \cdot min(1, \rho_{0d}^{-\alpha} e^{-\gamma \rho_{0d}})}{\lambda W_2 N_0 + I'}$.

Then the transmission rate of downlink over Rician fading channel is $\Theta\big(\log(e^{\frac{s^2}{\delta^2}} \epsilon \frac{n}{b})\big)$. Due to the bottleneck of downlink transmission, the transmission rate is then $R_{infra}^{Rician} = \Theta\big(\log(e^{\frac{s^2}{\delta^2}} \epsilon \frac{n}{b})\big)$. We complete the proof. ■

Lemma 12: While under *Nakagami-m* fading, as $n \to \infty$, the transmission rate of infrastructure mode from source node i to destination node j can be evaluated as follow

$$R_{infra}^{Nak} = \Theta\left(\log(\epsilon^{\frac{1}{m}} \frac{n}{b})\right) \ bit/s/Hz. \tag{23}$$

Proof: In terms of Nakagami-m fading, square magnitude $|h_{bj}|^2$ follows $\Gamma(m, \frac{1}{m})$ with a pdf of

$$f(x) = \frac{m^m}{\Gamma(m)} x^{m-1} e^{-mx}, \quad x \geq 0 \tag{24}$$

Applying (24), we have the outage performance for Nakagami-m fading scenario at high SNIR,

$$P'_{out} = \frac{m^m}{m!} \left[\frac{(2^R - 1)}{SNIR'}\right]^m \tag{25}$$

Solving $P'_{out} = \epsilon$, we have

$$C_{\epsilon}^{Nak'} = \log\left\{1 + \frac{1}{m}(m!)^{\frac{1}{m}} \cdot \epsilon^{\frac{1}{m}} \cdot SNIR'\right\}. \tag{26}$$

Then the transmission rate of downlink over Nakagami-m fading channel is $\Theta\big(\log(\epsilon^{\frac{1}{m}} \frac{n}{b})\big)$. Similarly, due to the limitation of downlink transmission, the transmission is then $\Theta\big(\log(\epsilon^{\frac{1}{m}} \frac{n}{b})\big)$. The proof is complete. ■

Several simulations will be provided to illustrate the bottleneck of the transmission under infrastructure mode. As shown in Figure 7, when outage probability ϵ is smaller, the of uplink throughput over Rician fading show its more prominently advantage. This conclusion further verifies the advantage of introducing opportunistic sources to the infrastructure mode and downlink phase has thus became the bottleneck of such mode. Note that, with the same ϵ, large Rician factor K ($K = 12$ dB) will improve the throughput of the downlink phase (21); and Moreover, as we have discussed in the uplink phase, the introduction of opportunistic sources will mitigate the dominant LOS transmission ($e^{\frac{s^2}{\delta^2}}$) of Rician fading. Thus, large Rician factor K narrows down the capacity difference between the the uplink and downlink phase.

Figure 8 illustrates the comparison between the throughput of both uplink and downlink over Nakagami-m fading. Clearly, as opportunistic sources number κ increases, the uplink throughput exceed the downlink scenario due to the benefit of opportunistic sources. Notice that the outage probability ϵ of both the uplink and downlink phase is weakened by Nakagami-m shape parameter m. Hence, large m narrows down the capacity difference between the the uplink and downlink phase.

V. CONCLUSION

In this paper, we investigated the outage throughput capacity bound of the hybrid wireless networks. For such hybrid networks with wired backbone, we examined the impact of different kind of fading and provided the close-form solutions for outage throughput capacity at high SNIR.

Opportunistic sources is introduced to cooperate with the scheduled source for intra-cell transmission mode where the bandwidth is shared by both kinds of the sources. Successive interference cancellation decoding scheme has been applied at receiver side in order to reduce the intra-cell interference and thus the maximum capacity can be achieved.

The outage throughput capacity under intra-cell transmission mode over Rayleigh, Rician and Nakagami-m fading are derived as $O\big(\log(\epsilon^{\frac{b}{n}} \frac{n}{b}) W_1\big)$, $O\big(\log[(e^{\frac{s^2}{\delta^2}} \epsilon)^{\frac{b}{n}} \frac{n}{b}] W_1\big)$ and $O\big(\log[(\epsilon^{\frac{1}{m}})^{\frac{b}{n}} \frac{n}{b}] W_1\big)$, respectively.

Clearly, by introducing the opportunistic sources, networks under intra-cell mode could effectively combat fading and the throughput capacity could therefore increasing significantly as the number of wireless nodes increases. However, downlink transmission would be the will be bottleneck of the infrastructure mode, since only the base station is transmitting data during the downlink phase. As for infrastructure transmission scenario, the corresponding outage throughput capacity over those three

fading channels are $\Theta\big(\frac{b}{n}\log(\epsilon\frac{n}{b})\,W_2\big)$,$\Theta\big(\frac{b}{n}\log(e^{\frac{s^2}{\delta^2}}\epsilon\frac{n}{b})\,W_2\big)$ and $\Theta\big(\frac{b}{n}\log(\epsilon^{\frac{1}{m}}\frac{n}{b})\,W_2\big)$, respectively.

APPENDIXES

APPENDIX A
PROOF OF LEMMA 8

Rician fading is the most applicable fading model when there exists a dominant line-of-sight (LOS) path from the transmitter to the receiver. It is characterized by two component: direct power s^2 and scatter power δ^2. A useful parameter Rician factor K about Rician LOS property is defined by $K = 10\log\frac{s^2}{\delta^2}$ dB.

The pdf of Rician random variable $|h_{ij}|$ is

$$f(h) = \frac{2h}{\delta^2}I_0(\frac{2sh}{\delta^2})e^{-\frac{h^2+s^2}{\delta^2}}, \quad h \geq 0$$

where $I_0(\cdot)$ denotes the modified *Bessel function* of the first kind with order zero. Thus, $||h||^2$ is actually a *noncentral* χ^2 distribution with $2(\kappa+1)$ degrees of freedom. The density of noncentral χ^2 variable with $2L$ degrees of freedom is as follow

$$f(x) = \frac{1}{\delta^2}(\frac{x}{s^2})^{\frac{L-1}{2}}e^{-\frac{s^2+x}{\delta^2}}I_{L-1}(\frac{2s}{\delta^2}\sqrt{x}), \quad x \geq 0,$$

where

$$I_{L-1}(x) = \sum_{k=0}^{\infty}\frac{(\frac{x}{2})^{L-1+2k}}{k!\Gamma(L+k)}, \quad x \geq 0.$$

With Rician fading scenario, the outage performance (14) could be transformed into

$$\begin{aligned}P\{||h||^2 < T\} &= \int_0^T \frac{1}{\delta^2}(\frac{x}{s^2})^{\frac{L-1}{2}}e^{-\frac{s^2+x}{\delta^2}}I_{L-1}(\frac{2s}{\delta^2}\sqrt{x})dx\\ &\overset{(a)}{\simeq} \int_0^T \frac{1}{e^{\frac{s^2}{\delta^2}}(\delta^2)^L(L-1)!}e^{-\frac{x}{\delta^2}}x^{L-1}dx\\ &\overset{(b)}{=} \frac{1}{e^{\frac{s^2}{\delta^2}}(\delta^2)^L(L-1)!}\cdot(\frac{1}{\delta^2})^{-L}\gamma(L,\frac{1}{\delta^2}T)\\ &\overset{(c)}{=} e^{-\frac{s^2}{\delta^2}}\big[1-e^{-\frac{T}{\delta^2}}\sum_{i=0}^{L-1}\frac{(\frac{T}{\delta^2})^i}{i!}\big]\end{aligned}$$

where (a) follows that, when x is small, such as $0 < x \leq \sqrt{\alpha+1}$, $I_\alpha(x) \approx \frac{1}{\Gamma(\alpha+1)}(\frac{x}{2})^\alpha$; (b) follows the definition of lower incomplete gamma function; (c) follows that $\gamma(n,x) = (n-1)!\big[1-e^{-x}\sum_{i=0}^{n-1}\frac{x^i}{i!}\big]$ if n is integer.

The outage probability P_{out} for Rician fading scenario is

$$P_{out} = e^{-\frac{s^2}{\delta^2}}\left\{1-e^{-\frac{(2^R-1)}{SNIR\cdot\delta^2}}\sum_{i=0}^{\kappa}\frac{1}{i!}\big[\frac{(2^R-1)}{SNIR\cdot\delta^2}\big]^i\right\} \quad (27)$$

with $SNIR = \frac{P\cdot min(1,\rho_{0d}^{-\alpha}e^{-\gamma\rho_{0d}})}{W_1\ N_0+I}$.

The resulting outage capacity over Rician fading channel can be obtained by solving

$$e^{-\frac{s^2}{\delta^2}}\left\{1-e^{-\frac{(2^R-1)}{SNIR\cdot\delta^2}}\sum_{i=0}^{\kappa}\frac{1}{i!}\big[\frac{(2^R-1)}{SNIR\cdot\delta^2}\big]^i\right\} = \epsilon. \quad (28)$$

Similarly, for arbitrary κ, there's no close-form solution. Therefore, by approximating e^{-x} with 1 for small x, the outage performance can be drawn as follow:

$$P_{out} = \frac{1}{e^{\frac{s^2}{\delta^2}}(\delta^2)^{\kappa+1}(\kappa+1)!}\big[\frac{2^R-1}{SNIR}\big]^{\kappa+1} \quad (29)$$

since, for small T,

$$\begin{aligned}P\{||h||^2 < T\} &= \int_0^T \frac{1}{e^{\frac{s^2}{\delta^2}}(\delta^2)^L(L-1)!}x^{L-1}dx\\ &= \frac{1}{e^{\frac{s^2}{\delta^2}}(\delta^2)^L L!}T^L.\end{aligned}$$

Hence, at high SNIR, the outage probability over Rician fading is given by (29). Solving $P_{out} = \epsilon$, we reach the outage capacity for Rician fading scenario

$$C_\epsilon^{Rician} = \log\left\{1+\delta^2(e^{\frac{s^2}{\delta^2}})^{\frac{1}{\kappa+1}}\cdot[(\kappa+1)!]^{\kappa+1}\cdot\epsilon^{\frac{1}{\kappa+1}}\cdot SNIR\right\}. \quad (30)$$

Note that the above outage capacity is also the upper bound due to the approximation in (14). Together with $\kappa = \Theta(\frac{n}{b})$ and $I = \Theta\big((\frac{n}{b})^{1-\frac{\alpha}{2}}\big)$, the sum rate over Rician fading channels of the scheduled and opportunistic sources is $O\big(\log[(e^{\frac{s^2}{\delta^2}}\epsilon)^{\frac{b}{n}}\frac{n}{b}]\big)$.

APPENDIX B
PROOF OF LEMMA 9

Fading in the case of urban cities with closely spaced buildings can be modeled better with Nakagami-m fading. The pdf of Nakagami-m random variable $|h_{ij}|$ is given by

$$f(h) = \frac{2}{\Gamma(m)}(\frac{m}{\Omega})^m h^{2m-1}e^{-mh^2/\Omega}, \quad h \geq 0 \quad (31)$$

where $\Gamma(\cdot)$ denotes the Gamma function, $\Omega = E[h^2]$ is the controlling spread and $m = \frac{E^2[h^2]}{Var[h^2]}$ is the shape parameter. For Nakagami-m fading, $\Omega = E[|h_{ij}|^2] = 1$. Clearly, $|h_{ij}|^2$ is distributed by

$$f(x) = \frac{m^m}{\Gamma(m)}x^{m-1}e^{-mx}, \quad x \geq 0 \quad (32)$$

which is actually a Gamma distribution. Since a random variable that follows Gamma-distribution with parameter (k,θ) can be formulated as

$$\Gamma(k,\theta) = \frac{1}{\theta^k}\frac{1}{\Gamma(k)}x^{k-1}e^{-\frac{x}{\theta}}, \quad x \geq 0,$$

we have $|h_{ij}|^2 \sim \Gamma(m,\frac{1}{m})$.

Here, we assume m is integer for purposes of analysis. Now the question is how is $||h||^2 = \sum_{i=0}^{\kappa}|h_{ij}|^2$ distributed?

From Lemma 13, we conclude that $||h||^2$ is another gamma-distribution with parameter $\big((\kappa+1)m,\frac{1}{m}\big)$. Its pdf is shown as follow

$$f(x) = \frac{m^{(\kappa+1)m}}{\Gamma[(\kappa+1)m]}x^{(\kappa+1)m-1}e^{-mx}. \quad (33)$$

Applying (33) into (14), we have

$$P\{||h||^2 < T\} = \frac{m^{(\kappa+1)m}}{\Gamma[(\kappa+1)m]}\int_0^T x^{(\kappa+1)m-1}e^{-mx}dx = \frac{m^{(\kappa+1)m}}{\Gamma[(\kappa+1)m]}\cdot m^{-(\kappa+1)m}\gamma\Big((\kappa+1)m, mT\Big) = 1 - e^{-mT}\sum_{i=0}^{(\kappa+1)m-1}\frac{(mT)^i}{i!}$$

By solving the following equation, the outage capacity over Rician fading can be calculated

$$1 - e^{-\frac{m(2^R-1)}{SNIR}}\sum_{i=0}^{(\kappa+1)m-1}\frac{[\frac{m(2^R-1)}{SNIR}]^i}{i!} = \epsilon. \tag{34}$$

Similarly, for arbitrary κ and m, there's no close-form solution. Approximating e^{-x} with 1 for small x, the outage performance at high SNIR can be examined as follow:

$$P_{out} = \frac{m^{(\kappa+1)m}}{[(\kappa+1)m]!}[\frac{(2^R-1)}{SNIR}]^{(\kappa+1)m} \tag{35}$$

since, according to (14), when T is small

$$P\{||h||^2 < T\} = \int_0^T \frac{m^{(\kappa+1)m}}{\Gamma[(\kappa+1)m]}x^{(\kappa+1)m-1}dx = \frac{m^{(\kappa+1)m}}{[(\kappa+1)m]!}T^{(\kappa+1)m}.$$

Solving $P_{out} = \epsilon$, we arrive at the outage capacity for Nakagami-m fading scenario

$$C_\epsilon^{Nak} = \log\left\{1 + \frac{1}{m}\cdot\epsilon^{\frac{1}{(\kappa+1)m}}\cdot[(\kappa+1)m]!^{\frac{1}{(\kappa+1)m}}\cdot SNIR\right\}. \tag{36}$$

Note that $\frac{1}{m}[(\kappa+1)m]!^{\frac{1}{(\kappa+1)m}} = \Theta(\frac{n}{b})$. Because the above outage capacity is the upper bound due to the approximation in (14), the sum rate of the scheduled and opportunistic sources over Nakagami-m fading Channels is $O\big(\log[(\epsilon^{\frac{1}{m}})^{\frac{b}{n}}\frac{n}{b}]\big)$. We complete the proof.

APPENDIX C
PROOF OF LEMMA 13

Lemma 13: If X_i, $i = 1, 2, ..., N$ follow independently gamma-distribution $\Gamma(k_i, \theta)$, we have

$$\sum_{i=1}^N X_i \sim \Gamma\Big(\sum_{i=1}^N k_i, \theta\Big). \tag{37}$$

Proof: The corresponding moment generating function (MGF) $M_x(t)$ is defined by

$$M_x(t) = E[e^{tx}] = \int_0^\infty e^{tx}f(x)dx \tag{38}$$

then for $Y = \sum_{i=1}^n X_i$, the MGF is

$$M_y(t) = E[e^{ty}] = E[e^{t(x_1+x_2+...x_n)}] = E[e^{tx_1}]E[e^{tx_2}]\cdots E[e^{tx_n}] = M_{x_1}(t)M_{x_2}(t)\cdots M_{x_n}(t) = \prod_{i=1}^n M_{x_i}(t)$$

As for Gamma distribution $\Gamma(k_i, \theta)$, $M_x(t) = \frac{1}{(1-\theta t)^{k_i}}$; thus the MGF of the sum of x_i is

$$M_y(t) = \frac{1}{(1-\theta t)^{\sum_{i=1}^n k_i}}, \tag{39}$$

which is clearly a MGF of a gamma-distribution $\Gamma(k', \theta')$ where $k' = \sum_{i=1}^n k_i$, $\theta' = \theta$. Thus $\sum_{i=1}^N X_i \sim \Gamma\big(\sum_{i=1}^N k_i, \theta\big)$. The proof is complete. ■

REFERENCES

[1] X. Wang and Q. Liang, "On the outage throughput capacity of hybrid wireless networks over fading channels," in *Proc. IEEE Globecom*, Anaheim, CA, USA, Dec. 2012, pp. 2173–2178.
[2] X. Wang, "Hybrid smart grid wireless networks: Capacity optimization," Ph.D Dissertation, Univ. Texas Arlington, Arlington, TX, USA, 2014.
[3] X. Wang and Q. Liang, "On the throughput capacity and performance analysis of hybrid wireless networks over fading channels," *IEEE Trans. Wireless Commun.*, vol. 12, no. 6, pp. 2930–2940, Jun. 2013.
[4] P. T. O. Dousse and M. Hasler, "Connectivity in ad-hoc and hybrid networks," in *Proc. IEEE INFOCOM*, Jun. 2002, pp. 1079–1088.
[5] P. Gupta and P. R. Kumar, "The capacity of wireless networks," *IEEE Trans. Inf. Theory*, vol. 46, no. 2, pp. 388–404, Mar. 2000.
[6] L.-L. Xie and P. R. Kumar, "A network information theory for wireless communication: Scaling laws and optimal operation," *IEEE Trans. Inf. Theory*, vol. 50, no. 5, pp. 748–767, May 2004.
[7] M. Franceschetti, O. Dousse, D. N. C. Tse, and P. Thiran, "Closing the gap in the capacity of wireless networks via percolation theory," *IEEE Trans. Inf. Theory*, vol. 53, no. 3, pp. 1009–1018, Mar. 2007.
[8] M. Grossglauser and D. Tse, "Mobility increases the capacity of ad-hoc wireless networks," *IEEE/ACM Trans. Netw.*, vol. 10, no. 4, pp. 477–486, Aug. 2002.
[9] K. Lu, J. Wang, L. Huang, and D. O. Wu, "On the throughput capacity of wireless sensor networks with mobile relays," *IEEE Trans. Veh. Technol.*, vol. 61, no. 4, pp. 1801–1809, May 2012.
[10] A. Ozgur, O. Leveque, and D. Tse, "Hierarchical cooperation achieves linear capacity scaling in ad hoc networks," in *Proc. IEEE INFOCOM*, May 2007, pp. 382–390.
[11] X. Y. Li, "Multicast capacity of wireless ad hoc networks," *IEEE/ACM Trans. Netw.*, vol. 17, no. 3, pp. 950–961, Jun. 2009.
[12] C. Wang, S. Tang, X. Li, and C. Jiang, "Multicast capacity scaling laws for multihop cognitive networks," *IEEE Trans. Mobile Comput.*, vol. 11, no. 11, pp. 1627–1639, Nov. 2011.
[13] Z. Li and B. Li, "Improving throughput in multihop wireless networks," *IEEE Trans. Veh. Technol.*, vol. 55, no. 3, pp. 762–773, May 2006.
[14] X.-Y. Li, S.-J. Tang, and O. Frieder, "Multicast capacity for large scale wireless ad hoc networks," in *Proc. ACM MobiHoc*, Montreal, QC, Canada, Sep. 2007.
[15] X. Mao, X.-Y. Li, and S.-J. Tang, "Multicast capacity for hybrid wireless networks," in *Proc. ACM MobiHoc*, Hongkong, 2008.
[16] B. Liu, Z. Liu, and D. Towsley, "On the capacity of hybrid wireless networks," in *Proc. INFOCOM*, vol. 2, Apr. 2003, pp. 1543–1552.
[17] U. C. Kozat and L. Tassiulas, "Throughput capacity of random ad hoc networks with infrastructure support," in *Proc. OBICOM*, 2003, pp. 55–65.
[18] A. Zemlianov and G. D. Veciana, "Capacity of ad hoc wireless networks with infrastructure support," *IEEE J. Sel. Areas Commun.*, vol. 23, no. 3, pp. 657–667, Mar. 2005.

[19] D. Kirachaiwanich and Q. Liang, "Capacity of wireless hybrid networks with successive interference cancellation," in *Proc. Globecom*, Dec. 2010, pp. 1–5.
[20] B. Liu, P. Thiran, and D. Towsley, "Capacity of wireless ad hoc network with with infrastructure," in *Proc. ACM MobiHoc*, Montreal, QC, Canada, Sep. 2007.
[21] W. Fu and D. P. Agrawal, "Capacity of hybrid wireless mesh networks with random APs," *IEEE Trans. Mobile Comput.*, vol. 12, no. 1, pp. 136–150, Jan. 2013.
[22] P. Zhou, X. Wang, and R. Rao, "Asymptotic capacity of infrastructure wireless mesh networks," *IEEE Trans. Mobile Comput.*, vol. 7, no. 8, pp. 1011–1024, Aug. 2008.
[23] G. Zhang, Y. Xu, X. Wang, and M. Guizani, "Capacity of hybrid wireless networks with directional antenna and delay constraint," *IEEE Trans. Commun.*, vol. 58, no. 7, pp. 2097–2106, Jul. 2010.
[24] F. Xue, L.-L. Xie, and P. R. Kumar, "The transport capacity of wireless networks over fading channels," *IEEE Trans. Inf. Theory*, vol. 51, no. 3, pp. 834–847, Mar. 2005.
[25] T. Cover and J. Thomas, *Elements of Information Theory*, 2nd ed. Hoboken, NJ, USA: Wiley, 2006.
[26] D. Tse and P. Viswanath, *Fundamentals of Wireless Communication*. Cambridge, U.K.: Cambridge Univ. Press, 2005.
[27] S. P. Weber, J. G. Andrews, X. Yang, and G. de Veciana, "Transmission capacity of wireless ad hoc networks with successive interference cancellation," *IEEE Trans. Inf. Theory*, vol. 53, no. 8, pp. 2799–2814, Aug. 2007.
[28] T. Le and Y. Liu, "On the capacity of hybrid wireless networks with opportunistic routing," *EURASIP J. Wireless Commun. Netw.*, 2010, Art. no. 202197.
[29] J. Blomer and N. Jindal, "Transmission capacity of wireless ad hoc networks: Successive interference cancellation vs. joint detection," in *Proc. IEEE Intl. Conf. Commun.*, Dresden, Germany, Jun. 2009, pp. 1–5.
[30] T. S. Rappaport, *Wireless Communications: Principles and Practice*, 2nd ed. Upper Saddle River, NJ, USA: Prentice-Hall, 2002.
[31] J. G. Proaksi and M. Salehi, *Digtial Communication*, 5th ed. New York, NY, USA: McGraw-Hill, 2008.

XIN WANG received the Ph.D. degree in electrical engineering from The University of Texas at Arlington, in 2014. He is working with LinkedIn Corporation, Sunnyvale, CA, USA. He has published articles in prestigious journals, such as the IEEE TRANSACTIONS ON WIRELESS COMMUNICATIONS, the IEEE SYSTEMS JOURNAL, and in prestigious conferences, such as the IEEE ICC and GLOBECOM. His research interests are wireless communications, hybrid wireless networks, 5G new radio, and wireless sensor networks. He was the Chair of the IEEE INFOCOM 2017 Workshop on 5G New Radio Technologies and the IEEE INFOCOM 2016 Workshop on 5G & Beyond—Enabling Technologies and Applications. He served as a Guest Editor for the IEEE INTERNET OF THINGS JOURNAL, IEEE ACCESS, *Physical Communication*, *Mobile Information Systems*, and *Ad Hoc Network*.

ZIKAI WANG received the B.S. degree from the Beijing University of Posts and Telecommunications (BUPT), in 2015. He is currently pursuing the Ph.D. degree with the Department of Electrical Engineering, The University of Texas at Arlington. His current research interests include array signal processing, wireless communication, and information systems.

QILIAN LIANG received the B.S. degree from Wuhan University, in 1993, the M.S. degree from the Beijing University of Posts and Telecommunications (BUPT), in 1996, and Ph.D. degree from the University of Southern California (USC), in 2000, all in electrical engineering. He is currently a Distinguished University Professor with the Department of Electrical Engineering, The University of Texas at Arlington (UTA). Prior to joining the faculty of The University of Texas at Arlington in August 2002, he was a Member of Technical Staff at Hughes Network Systems Inc., San Diego, California. He has published more than 320 journals and conference papers and seven book chapters. His research interests include wireless sensor networks, radar and sonar sensor networks, wireless communications and networks, signal processing, and machine learning. He received the 2002 IEEE Transactions on Fuzzy Systems Outstanding Paper Award, the 2003 U.S. Office of Naval Research (ONR) Young Investigator Award, the 2005 UTA College of Engineering Outstanding Young Faculty Award, the U.S. Air Force Summer Faculty Fellowship Program Award, in 2007, 2009, and 2010, the 2012 UTA College of Engineering Excellence in Research Award, and the 2013 UTA Outstanding Research Achievement Award. He was inducted into the UTA Academy of Distinguished Scholars, in 2015.